Available online at www.sciencedirect.com
SCIENCE DIRECT
Journal of Power Sources 151 (2005) 74–78
JOURNAL OF POWER SOURCES
www.elsevier.com/locate/jpowsour

Short communication

Synthesis and electrical properties of new rare-earth titanium perovskites for SOFC anode applications

F.J. Lepe, J. Fernández-Urbán, L. Mestres*, M.L. Martínez-Sarrión

Departament de Química Inorgànica, Universitat de Barcelonam, c/. Martí i Franquès 1-11, E-08028 Barcelona, Spain

Accepted 4 February 2005
Available online 31 May 2005

Abstract

New oxides of general formula $Ln_{2/3-x}TiO_{3-3x/2}$ (Ln = La, Pr and Nd; $0.07 \leq x \leq 0.13$) have been prepared by a new synthetic route, starting with precursors $Ln_{2/3-x}Li_{3x}TiO_3$ with perovskite structure. Precursors were prepared by the ceramic method and a modified Pechini sol–gel process, and both were treated with nitric acid 2 M to exchange lithium ions by protons, leading to new phases $Ln_{2/3-x}TiO_{3-3x}(OH)_{3x}$. These phases were calcined in order to dehydrate them and obtain the anion defect oxides $Ln_{2/3-x}TiO_{3-3x/2}$. All the phases showed perovskite-type X-ray powder diffraction patterns during the successive steps of the synthesis. Anionic vacancy content was calculated by an indirect method, taking into consideration the metallic relation, determined by induced coupled plasma (ICP), and the absence of Ti(III), checked by electron paramagnetic resonance (EPR). AC electric measurements carried out under different atmospheres (N_2, Ar, H_2/Ar, air and O_2) showed a conductivity increase under reducing atmosphere, due to the reduction of Ti(IV) to Ti(III). Considering their electrical behavior, these new phases become candidates for solid oxide fuel cell (SOFC) anode materials.

Keywords: SOFC; Sol–gel process; Perovskites; Electrical properties; Impedance spectroscopy

1. Introduction

Perovskite oxides have some quite interesting properties, such as ionic conductivity [1], superconductivity [2], magnetorresistance [3] and ferroelectricity [4]. In solid oxide fuel cells (SOFCs), perovskites such as strontium and magnesium doped $LaGaO_3$ exhibit high oxygen ionic conductivity and have been well studied as electrolytes [5,6]. Other perovskites with mixed conductivity like $La_{1-x}Sr_xMnO_3$ and $La_{1-x}Sr_xCo_{1-x}O_3$ have been used as SOFC cathodes [7,8]. Another perovskite compound with only electronic conductivity, $La_{1-x}M_xCrO_3$ (M = Ca and Sr), has been investigated as an interconnector for SOFCs [7]. Perovskites have also been studied as potential SOFC anodes. The principle requirements for this use are electronic conductivity and chemical stability under reducing conditions. Chromium and titanium based perovskites are the most promising SOFC anode materials, especially lanthanum strontium titanates [9–11].

The synthesis of new perovskites with oxygen vacancies under non-drastic conditions is a challenge for solid-state chemistry. The use of ionic exchange reactions followed by thermal treatments to obtain metastable phases is well known [12,13], and more recently this method has been used to synthesize other perovskites [14,15]. The principle requirement for this kind of reactions is high ionic mobility in the starting compounds. There is no change in the structure due to the different ions in the lattice after the reaction. This is the case in lanthanum lithium titanates, which have high lithium conductivity [16,17] and no structure variation after the ionic exchange, as reported in tetragonal $La_{2/3-x}Li_{3x}TiO_3$ [18]. In the present study, the conditions of the synthesis for other rare-earth lithium titanates, with perovskite cubic structure, have been established, and the electrical behavior of these compounds for their use as SOFC anodes has been examined.

* Corresponding author. Tel.: +34 934037057; fax: +34 934907725.
E-mail address: lourdes.mestres@qi.ub.es (L. Mestres).

0378-7753/$ – see front matter © 2005 Elsevier B.V. All rights reserved.
doi:10.1016/j.jpowsour.2005.02.087

2. Experimental

New perovskites $Ln_{2/3-x}TiO_{3-3x/2}$ (Ln = La, Pr and Nd; $0.07 \leq x \leq 0.13$) were prepared by lithium exchange of $Ln_{2/3-x}Li_{3x}TiO_3$ precursors followed by dehydration and calcination steps. Precursors were prepared by two methods: ceramic and sol–gel. In the ceramic route [19,20], stoichiometric amounts of TiO_2 (Aldrich 99.9%), La_2O_3 (Fluka 99.98%), $Ce_2(CO_3)_3{\cdot}5H_2O$ (Aldrich 99.9%), Pr_6O_{11} (Aldrich 99.9%) and Nd_2O_3 (Aldrich 99.9%), were intimately mixed with acetone. Oxide reagents were previously dried overnight at 900 °C. The mixture was dried and heated to 650 °C for 3 h to drive off CO_2, and then pressed into pellets and covered with powder of the same composition to avoid loss of lithium during thermal treatment. The pellets were fired at 1100, 1200 and 1250 °C for 15 h with intermediate grinding and re-pelleting. Each treatment finished with quenching to room temperature. The sol–gel method was a modification of the Pechini process [21,22] as shown in Fig. 1. The reagents used were $La(NO_3)_3{\cdot}6H_2O$ (Aldrich 99.9%), $Ce(NO_3)_3{\cdot}6H_2O$ (Avocado 99.5%), Pr_6O_{11} (Aldrich 99.9%) and Nd_2O_3 (Aldrich 99.9%), depending on the rare-earth, $LiNO_3$ (Aldrich QP), a 0.5 M aqueous solution of $TiOCl_2$ (Millenium Chemicals 99.5%), citric acid (BDH 99.7%) and ethyleneglycol (Probus QP). Stoichiometric amounts of the rare-earth compound and $LiNO_3$ were weighed and solved separately in the minimum amount of water. Pr and Nd oxides were previously solved into an HNO_3 10% solution. The two aqueous solutions were mixed and the metals were complexed with a solution of citric acid in the minimum amount of water, in a ratio citric acid:metal ions of 2:1. The necessary volume of $TiOCl_2$ 0.5 M was added to this solution. Finally, ethyleneglycol was added in a molar ratio 60:40 with respect to citric acid. The solution was stirred for an hour, and then heated to 60 °C to reduce the volume until polymerization was observed and an aerogel was obtained. Gels were aged at 120 °C for 15 h and fired at 1100 °C at a heating rate of 1 °C min^{-1}, and this temperature was kept for 15 h. Finally, the samples were quenched to room temperature. X-ray diffraction analysis showed the absence of perovskite formation in cerium compounds.

Lithium exchange conditions previously reported for the preparation of $La_{2/3-x}TiO_{3-3x}(OH)_{3x}$ powders [18,23] were optimized for densified $Ln_{2/3-x}TiO_{3-3x}(OH)_{3x}$ samples (Ln = La, Pr and Nd). Pellets with 6 mm diameter and 2 mm thickness were sintered at 1250 °C for 1 h. Sintered pellets were stirred and heated to 90 °C for a period of between 7 and 10 days with an appropriate volume of nitric acid 2 M to give a proton:lithium ratio of 100:1 in a closed system. Finally, the optimal conditions for dehydration were found to be heating from room temperature to 950 °C at 1 °C min^{-1} under nitrogen atmosphere, and then holding at 950 °C for 60 h in the same conditions, ending with quenching to room temperature.

Powder X-ray diffraction patterns were collected with a Siemens D-500 diffractometer with Bragg Brentano geometry, using Cu Kα radiation at 40 kV and 30 mV, and recorded over an angular range of 4.0°–70.0° with a 0.05° step-size. Phase identification was performed with DRXWin program [24], including Creafit software. Lattice parameters were calculated with the *Fullprof* software [25]. Metal atomic content was determined by atomic emission spectroscopy by induced coupled plasma (AES-ICP) using an emission spectrometer Perkin-Elmer optima 3200 RL. Electron paramagnetic resonance (EPR) studies were carried out with a Bruker 300-E automatic spectrometer in the X-band (9.45 GHz). Temperature was controlled with a quartz cryostat with liquid nitrogen in order to measure spectra from 77 K to room temperature. AC electric measurements were carried out using a HP4192A impedance analyzer over a frequency range from 5 Hz to 13 MHz under different atmospheres (N_2, Ar, H_2/Ar, air and O_2). Data were analyzed by *Zview*2 software [26].

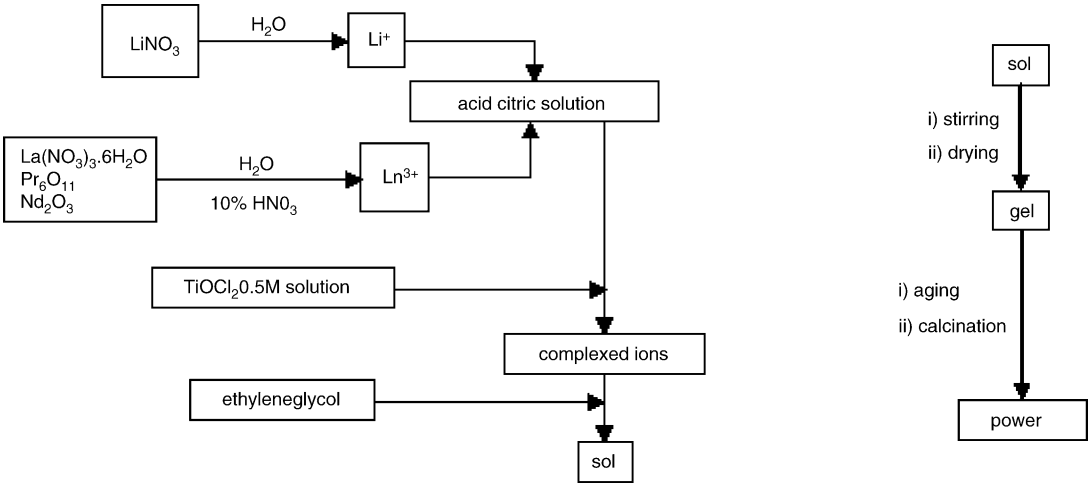

Fig. 1. Flux diagram of sol–gel method synthetic route.

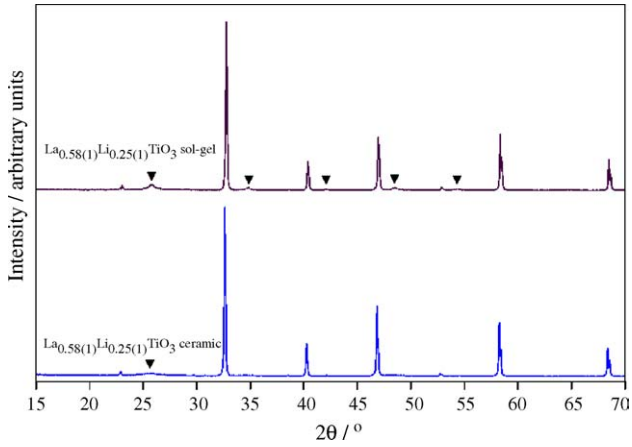

Fig. 2. XRD patterns of $La_{0.58(1)}Li_{0.25(1)}TiO_3$ obtained by ceramic and sol–gel methods. Tetragonal phase broad peaks are marked with ▼.

Table 1
Experimental formulae of compounds synthesized

Precursors	Exchanged compounds	Dehydrated compounds
$La_{0.60(1)}Li_{0.21(1)}TiO_3$	$La_{0.60(1)}TiO_{2.79}(OH)_{0.21}$	$La_{0.60(1)}TiO_{2.90}$
$La_{0.58(1)}Li_{0.25(1)}TiO_3$	$La_{0.58(1)}TiO_{2.75}(OH)_{0.25}$	$La_{0.58(1)}TiO_{2.87}$
$La_{0.57(1)}Li_{0.29(1)}TiO_3$	$La_{0.57(1)}TiO_{2.71}(OH)_{0.29}$	$La_{0.57(1)}TiO_{2.86}$
$La_{0.55(1)}Li_{0.34(1)}TiO_3$	$La_{0.55(1)}TiO_{2.66}(OH)_{0.34}$	$La_{0.55(1)}TiO_{2.83}$
$La_{0.54(1)}Li_{0.39(1)}TiO_3$	$La_{0.54(1)}TiO_{2.61}(OH)_{0.39}$	$La_{0.54(1)}TiO_{2.81}$
$Pr_{0.60(1)}Li_{0.21(1)}TiO_3$	$Pr_{0.60(1)}TiO_{2.79}(OH)_{0.21}$	$Pr_{0.60(1)}TiO_{2.90}$
$Pr_{0.58(1)}Li_{0.25(1)}TiO_3$	$Pr_{0.58(1)}TiO_{2.75}(OH)_{0.25}$	$Pr_{0.58(1)}TiO_{2.87}$
$Pr_{0.57(1)}Li_{0.29(1)}TiO_3$	$Pr_{0.57(1)}TiO_{2.71}(OH)_{0.29}$	$Pr_{0.57(1)}TiO_{2.86}$
$Pr_{0.55(1)}Li_{0.34(1)}TiO_3$	$Pr_{0.55(1)}TiO_{2.66}(OH)_{0.34}$	$Pr_{0.55(1)}TiO_{2.83}$
$Pr_{0.54(1)}Li_{0.39(1)}TiO_3$	$Pr_{0.54(1)}TiO_{2.61}(OH)_{0.39}$	$Pr_{0.54(1)}TiO_{2.81}$
$Nd_{0.60(1)}Li_{0.21(1)}TiO_3$	$Nd_{0.60(1)}TiO_{2.79}(OH)_{0.21}$	$Nd_{0.60(1)}TiO_{2.90}$
$Nd_{0.58(1)}Li_{0.25(1)}TiO_3$	$Nd_{0.58(1)}TiO_{2.75}(OH)_{0.25}$	$Nd_{0.58(1)}TiO_{2.87}$
$Nd_{0.57(1)}Li_{0.29(1)}TiO_3$	$Nd_{0.57(1)}TiO_{2.71}(OH)_{0.29}$	$Nd_{0.57(1)}TiO_{2.86}$
$Nd_{0.55(1)}Li_{0.34(1)}TiO_3$	$Nd_{0.55(1)}TiO_{2.66}(OH)_{0.34}$	$Nd_{0.55(1)}TiO_{2.83}$
$Nd_{0.54(1)}Li_{0.39(1)}TiO_3$	$Nd_{0.54(1)}TiO_{2.61}(OH)_{0.39}$	$Nd_{0.54(1)}TiO_{2.81}$

3. Results and discussion

X-ray diffraction data of the precursors obtained by the two methods show that all compounds have a *Pm*3*m* cubic structure, with the presence of some broad peaks of the tetragonal *P4/mmm* phase [19,20]. The tetragonal phase is more obviously observed in sol–gel samples, as illustrated in Fig. 2, because the synthesis temperature was lower. Cerium perovskites are the exception because they were not obtained in these conditions. Comparison of XRD patterns of the precursors, ionic exchanged samples and final compounds shows that there is no change in the structure due to the different processes that involve the synthesis (Fig. 3). Variations in cell parameters during the process are small, in the order of 0.01 Å.

The formulae of compounds synthesized are shown in Table 1. Formulae include experimental error in metal determination by AES-ICP, considering that titanium is always in Ti(IV) oxidation state and that one proton substitutes one lithium ion. Results are identical for ceramic and sol–gel precursors. The absence of lithium in ionic exchanged samples is verified also with AES-ICP. Proton presence is observed in ^{1}H-MAS-NMR, as in previous work [18]. Further studies in quantification of protons in these samples by NMR will be done. The absence of Ti(III) in dehydrated compounds was checked by EPR and spectra like Fig. 4 were obtained with lanthanum compounds. Spectral shape does not change with temperature and it shows only one signal, centered at $g = 2.000$ and only 10G wide. This signal is typical of organic radicals, but in this case it is due to the presence of electrons trapped in anionic vacancies, as in natural quartz [27]. Praseodymium and neodymium are difficult to study by EPR, since they have f electrons that interfere with the technique.

$Ln_{2/3-x}TiO_{3-3x/2}$ (Ln = La and Pr) samples were studied by impedance spectroscopy. Bulk conductivity values of the samples under nitrogen atmosphere are shown in Table 2. Grain boundary resistance values are three orders of magnitude higher than bulk values. $La_{0.60(1)}TiO_{2.90}$ and $Pr_{0.60(1)}TiO_{2.90}$ samples have the best conductivity values. Fig. 5 shows the electrical behavior of these two samples in

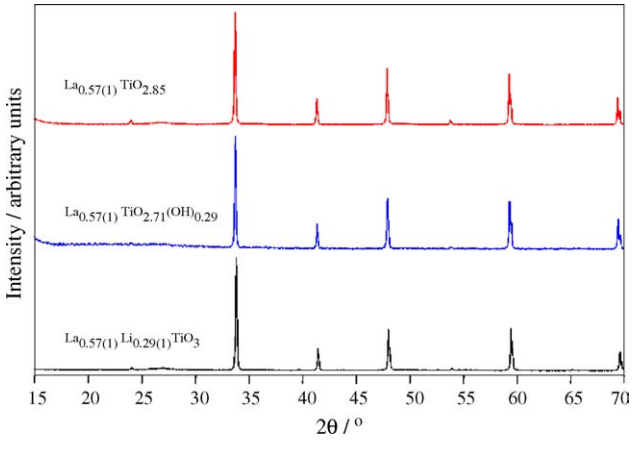

Fig. 3. XRD patterns of $La_{0.57(1)}Li_{0.29(1)}TiO_3$, $La_{0.57(1)}TiO_{2.71}(OH)_{0.29}$ and $La_{0.57(1)}TiO_{2.85}$.

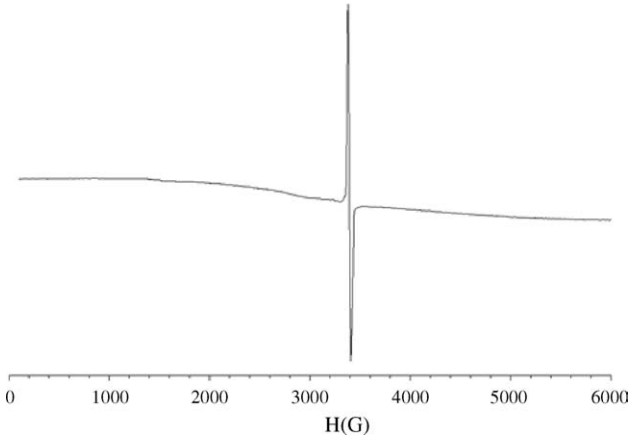

Fig. 4. EPR spectrum of $La_{0.60(1)}TiO_{2.90}$ at 77 K.

Table 2
Bulk conductivity values at 423 K under N_2, activation energies and densification degrees of lanthanum and praseodymium samples

La samples	Bulk σ (S cm^{-1}) at 423 K	Praseodymium samples	Bulk σ (S cm^{-1}) at 423 K
$La_{0.60(1)}TiO_{2.90}$	1.30×10^{-4}	$Pr_{0.60(1)}TiO_{2.90}$	1.65×10^{-5}
$La_{0.58(1)}TiO_{2.87}$	1.10×10^{-4}	$Pr_{0.58(1)}TiO_{2.87}$	1.42×10^{-5}
$La_{0.57(1)}TiO_{2.86}$	1.00×10^{-4}	$Pr_{0.57(1)}TiO_{2.86}$	1.27×10^{-5}
$La_{0.55(1)}TiO_{2.83}$	8.25×10^{-5}	$Pr_{0.55(1)}TiO_{2.83}$	1.10×10^{-5}
$La_{0.54(1)}TiO_{2.81}$	7.35×10^{-5}	$Pr_{0.54(1)}TiO_{2.81}$	9.75×10^{-6}

La samples	Ea (eV)	Densification (%)	Praseodymium samples	Ea (eV)	Densification (%)
$La_{0.60(1)}TiO_{2.90}$	0.42	61	$Pr_{0.60(1)}TiO_{2.90}$	0.54	60
$La_{0.58(1)}TiO_{2.87}$	0.43	58	$Pr_{0.58(1)}TiO_{2.87}$	0.55	57
$La_{0.57(1)}TiO_{2.86}$	0.45	56	$Pr_{0.57(1)}TiO_{2.86}$	0.56	54
$La_{0.55(1)}TiO_{2.83}$	0.47	54	$Pr_{0.55(1)}TiO_{2.83}$	0.58	52
$La_{0.54(1)}TiO_{2.81}$	0.48	52	$Pr_{0.54(1)}TiO_{2.81}$	0.59	50

these conditions. The grain contribution is much smaller than the grain boundary contribution and cannot be observed. The semicircles are assigned to these contributions by their capacity values, $\sim 10^{-11}$ F for grain and $\sim 10^{-9}$ F for grain boundary [28]. Grain and grain boundary resistances are lower for lanthanum compounds than for praseodymium. This can be due to little structural differences because praseodymium compounds diffraction data show more presence of broad peaks attributed to the tetragonal phase. There is no change between heating and cooling measurements and the compounds act as semiconductors. Under oxygen-rich atmospheres, the same tendency is observed. Differences in conductivity between different samples with the same lanthanide are small and can be attributed to differences in the degree of densification. These values range from 60 to 50% with oxygen vacancy increase, relating poor densification with high oxygen vacancy presence.

When the same comparison is done under 5% hydrogen in argon, the result is the same (Fig. 6), except for the resistance values, which are lower for both lanthanum and praseodymium compounds. Decrease in the resistance values is due to the greater presence of charge carriers in these conditions, since hydrogen can reduce Ti(IV) to Ti(III), providing electrons with high mobility in the structure by a hopping mechanism. Differences between lanthanum and praseodymium compounds arise when cooling spectra are compared. Fig. 7 shows this tendency. Grain boundary resistance is lower for praseodymium than for lanthanum, in contrast to the behavior observed in the heating spectra. Arrhenius plots for bulk conductivity in cooling measurements are presented in Fig. 8. Bulk activation energies of the compounds presented in this figure are 0.42 eV for lanthanum and 0.54 eV for praseodymium. Bulk conductivity is always better for lanthanum compounds than for praseodymium, but grain boundary resistance is lower for praseodymium compounds. Grain boundary activation energy is similar for both compounds, around 1.41 eV. The explanation for the change in the behavior of the grain boundary of praseodymium samples will require more accurate studies.

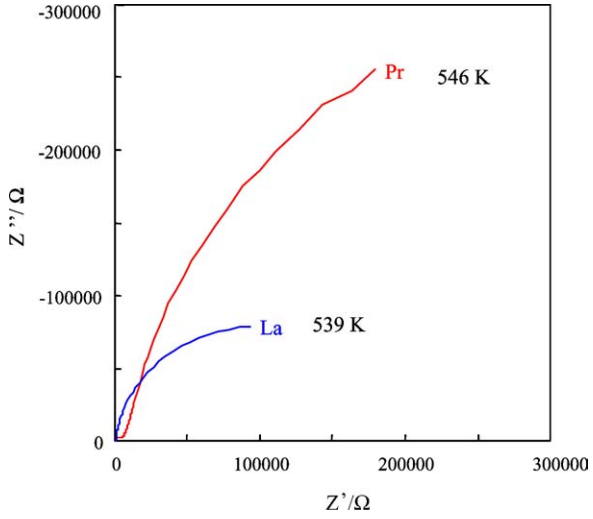

Fig. 5. Comparison of electrical behavior of $La_{0.60(1)}TiO_{2.90}$ and $Pr_{0.60(1)}TiO_{2.90}$ under N_2.

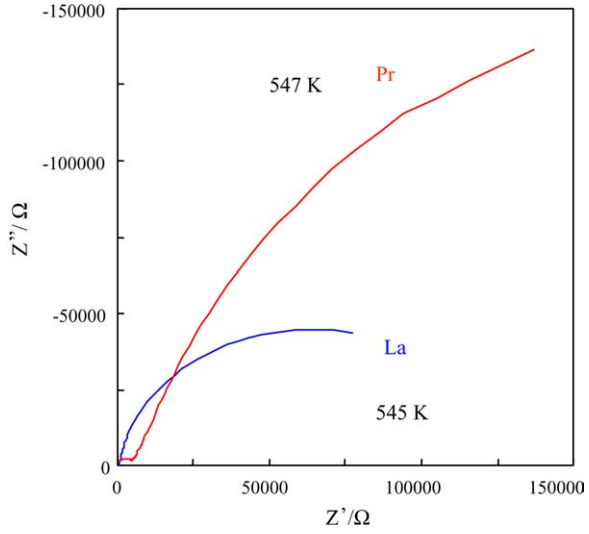

Fig. 6. Comparison of electrical behavior of $La_{0.60(1)}TiO_{2.90}$ and $Pr_{0.60(1)}TiO_{2.90}$ under 5 %H_2/Ar in heating conditions.

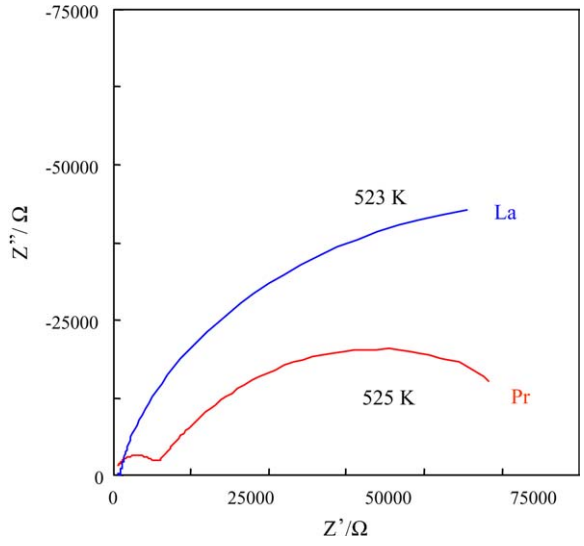

Fig. 7. Comparison of electrical behavior of $La_{0.60(1)}TiO_{2.90}$ and $Pr_{0.60(1)}TiO_{2.90}$ under 5 %H_2/Ar in cooling conditions.

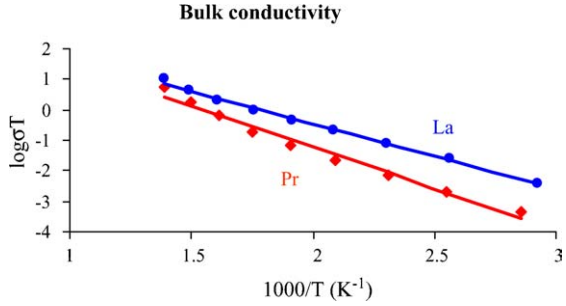

Fig. 8. Arrhenius plots of $La_{0.60(1)}TiO_{2.90}$ and $Pr_{0.60(1)}TiO_{2.90}$ bulk conductivity under 5 %H_2/Ar in cooling conditions.

4. Conclusions

Lanthanide titanium oxides $Ln_{2/3-x}TiO_{3-3x/2}$ (Ln = La, Pr and Nd) have been synthesized by a new synthetic route. All the different steps of the synthesis have been optimized to work with initial densified precursors and to obtain the better densification in final compounds. Precursors of general formula $Ln_{2/3-x}Li_{3x}TiO_3$ (Ln = La, Pr and Nd) have been obtained by a new sol–gel method, but not for cerium compositions. Electrical conductivities of $Ln_{2/3-x}TiO_{3-3x/2}$ (Ln = La and Pr) have been studied, showing an interesting behavior for $Pr_{2/3-x}TiO_{3-3x/2}$ in reducing conditions, which will be the subject of future studies. The electrical properties of these compounds indicate that they may become candidates for SOFC anodes.

Acknowledgments

This study received support from the Departament d' Universitats, Recerca i Societat de la Informació de la Generalitat de Catalunya and was sponsored by Ministerio de Ciencia y Tecnología (BQU2002-00619).

References

[1] Y. Inaguma, C. Liquan, M. Itoh, T. Nakamura, T. Uchida, H. Ikuta, M. Wakihara, Solid State Commun. 86 (1993) 689–693.
[2] H. Fukuoka, T. Isami, S. Yamanaka, Chem. Lett. 8 (1997) 703–704.
[3] Y. Moritomo, A. Asamitsu, H. Kuwahara, Y. Tokura, Nature 380 (1996) 141–144.
[4] W.A. Schulze, J.V. Biggers, L.E. Cross, J. Am. Ceram. Soc. 61 (1996) 46–49.
[5] T. Ishihara, H. Matsuda, Y. Takita, J. Am. Chem. Soc. 116 (1994) 3801–3803.
[6] T. Ishihara, H. Matsuda, Y. Takita, Solid State Ionics 79 (1995) 147–151.
[7] N.Q. Minh, J. Am. Ceram. Soc. 76 (1993) 563–588.
[8] H.Y. Tu, Y. Takeda, N. Imanishi, O. Yamamoto, Solid State Ionics 117 (1999) 277–281.
[9] G. Pudmich, B.A. Boukamp, M. Gonzalez-Cuenca, W. Jungen, W. Zipprich, F. Tietz, Solid State Ionics 135 (2000) 433–438.
[10] S. Primdahl, J.R. Hansen, L. Grahl-Madsen, P.H. Larsen, J. Electrochem. Soc. 148 (2001) A74–A81.
[11] O.A. Marina, N.L. Canfield, J.W. Stevenson, Solid State Ionics 135 (2002) 21–28.
[12] B. Gerand, G. Nowogrocki, J. Guenot, M. Figlarz, J. Solid State Chem. 29 (1979) 429–434.
[13] J. Gopalakrishnan, V. Bhat, Inorg. Chem. 26 (1987) 4299–4301.
[14] R. Marchand, L. Brohan, M. Tournoux, Mater. Res. Bull. 15 (1980) 1129–1133.
[15] K. Toda, S. Tokuoka, K. Uematsu, M. Sato, Solid State Ionics 154–155 (2002) 393–398.
[16] H. Kawai, J. Kuwano, J. Electrochem. Soc. 141 (1996) L78–L79.
[17] Y. Inaguma, M. Itoh, Solid State Ionics 86–88 (1996) 257–260.
[18] N.S.P. Bhuvanesh, O. Bohnké, H. Duroy, M.P. Crosnier-Lopez, J. Emery, J.L. Fourquet, Mater. Res. Bull. 33 (1998) 1681–1691.
[19] A.D. Robertson, S. Garcia Martin, A. Coats, A.R. West, J. Mater. Chem. 5 (1995) 1405–1412.
[20] M. Morales, A.R. West, Solid State Ionics 91 (1996) 33–43.
[21] M. Pechini, U.S. Patent 3,330,697, July 11, 1967.
[22] F. J. Lepe, C. Ostos, L. Mestres, M. L. Martínez-Sarrión, in press.
[23] L. Mestres, M.L. Martínez-Sarrión, F.J. Lepe, Boletín de la Sociedad Española de Cerámica y Vidrio 43 (2004) 764–768.
[24] V. Primo Martín, DRXWin and CreaFit 2.0: graphical and analytical tools for powder XRD patterns, Powder Diffr. 14 (1999) 70–73.
[25] J. Rodríguez-Carvajal, *Fullprof* 98, in: Laboratoire Léon Brillouin, CEA-Saclay, France, 2000.
[26] *Zview* 2 for Windows (Version 2.0), Scribner Assoc. Inc., Charlottesville, VA, USA, 2000.
[27] M. Ikeya, New Applications of Electron Spin Resonance, World Scientific, 1993.
[28] J.T.S. Irvine, D.C. Sinclair, A.R. West, Adv. Mater. 2 (1990) 132–138.